

51 2005) have progressed so much that it is reasonable to investigate new frontiers in the
52 application of driving simulators.

53 Here the authors present the first results of a driving simulation based study oriented to
54 analyze the engineering problems in the design and improvement of a Formula 1 or
55 competition circuit and in the optimization of the pilots' race performances. The optimization
56 of the circuit mostly depends on:

- 57 - physical – structural features: e.g. the impact speed in the case of run off accident,
- 58 - geometrical – perceptive features: e.g. the influence of geometrical standard, as radii
59 or lane dimension, on driving performances.

60

61 FIA has developed a specific software to improve the safety of the circuits related to the first
62 point: Circuit Analysis and Safety System (CSAS). CSAS is used to evaluate the effectiveness
63 of the run-off areas and protective measures, it means the passive safety of existing GP
64 circuits. The software integrates the circuit digital maps and some dynamical data acquired by
65 vehicular sensors. Finally CSAS predicts the severity of impacts in any circuit's point, basing
66 on the speed, deceleration data and passive measures characteristics. Actually the geometrical
67 – perceptive features are not in depth investigated. This paper gives a contribution to identify
68 novel proposals for optimizing the circuit and the pilots' performance.

69

70 The authors have used a STI driving simulator (Benedetto et al., 2002). The physical and
71 mechanical characteristics of the simulated vehicle have been improved in order to reproduce
72 as possible a competition vehicle. For the tests we have simulated the urban circuit of Rome
73 that has been recently proposed.

74

75 Two professional pilots have been requested to drive for the tests. Before the test a training
76 protocol has been implemented so that the pilots familiarize with the simulation environment.
77 Each pilot has driven for 15 laps during the test. During the tests we have observed an average
78 speed (Klee et al., 1999; Godley et al., 2002; Bella, 2008) of the best lap (134.86 km/h)
79 compatible with the speeds observed in analogous urban circuits (136.63 km/h Montecarlo
80 3340 m, 146.10 km/h Singapore 5073 m, 158.60 km/h Valencia 5419 m). After the tests the
81 time histories of longitudinal speed, longitudinal and transversal acceleration have been post
82 processed. Moreover the vehicle trajectory and lateral displacement have been analyzed on
83 the average and in the case of the best lap. Finally the used and available friction rate has been
84 studied following a two dimensional approach in the case of the most critical curves. In
85 particular three curves have been isolated as most critical being the rate between used and
86 available friction over 0.80. These mentioned rates have been visualized on the curves maps
87 so that the spatial distribution of used friction is in evidence.

88

89 **OBJECTIVE**

90

91 The overall objective of the paper is to investigate the applicability and the potentialities of
92 the driving simulation for Formula 1 circuits optimization, both in terms of geometry and in
93 terms of pavement friction. Moreover the paper presents the first results in order to
94 demonstrate the possible applications of driving simulator for improving the pilot
95 performances and for reducing the time laps.

96

97 **FIA REQUIREMENTS**

98

99 The FIA has published some requirements for assisting in the basic conception of circuit
100 projects for submission in view of future licensing. Here we have extracted and summarized

101 some of these main requirements, for completeness. In plan the shape of the course is not
102 restricted, but the FIA may recommend changes in the interests of good competition and from
103 practical necessity. The maximum permitted length for straight sections of track is 2km. The
104 maximum length (centerline) of any new circuit should not exceed 7 km. In general, unless
105 otherwise stated, all references to straights and curves concern the actual trajectory followed
106 by the cars with the highest performance and not the geometrical form of the layout. The track
107 width should be at least 12 m. Where the track width changes, the transition should be made
108 as gradually as possible, at a rate not greater than 1 m in 20 m total width. The width of the
109 starting grid should be at least 15 m.

111 Any change in gradient should be effected using a minimum vertical radius calculated by the
112 formula:

$$114 \quad R = V^2 \cdot K \quad (1)$$

116 where

- 117 - R is the radius in meters,
- 118 - V is the speed in kph and
- 119 - K is a constant equal to 20 in the case of a concave profile or to 15 in the case of a
120 convex profile.

122 The value of R should be adequately increased along approach, release, braking and curved
123 sections. Wherever possible, changes in gradient should be avoided altogether in these
124 sections. The gradient of the start/finish straight should not exceed 2%.

126 Along straights, the transversal incline, for drainage purposes, between the two edges of the
127 track or between the centerline and the edge (camber), should not exceed 3%, or be less than
128 1.5 %. In curves, the banking (downwards from the outside to the inside of the track) should
129 not exceed 10% (with possible exceptions in special cases, such as speedways).

131 A permanent track should be bordered along its entire length on both sides by continuous
132 white lines clearly marked in anti-skid paint, minimum 10 cm wide, and compact verges,
133 usually between 1 m and 5 m wide, having an even surface. A run-off area is an area of
134 ground between the verge and the first line of protection. A run-off area should be graded to
135 the verge. If the area has a slope, this should not exceed 25% upwards (does not apply to
136 gravel beds) or 3% downwards, with a smooth transition from track to run-off area, in relation
137 to the lateral projection of the track surface.

139 For standing starts, there should be at least 6 m length of grid per car (8 m for the Formula
140 One World Championship). There should preferably be at least 250 m between the starting
141 line and the first corner. By corner, in these cases only, is understood a change of direction of
142 at least 45°, with a radius of less than 300 m.

144 When determining measures intended for the protection of spectators, drivers, race officials
145 and service personnel during competitions, FIA recommends that the characteristics of the
146 course should be taken into consideration (track layout and profile, topography, racing
147 trajectories, adjacent areas, buildings and constructions) as well as the speed attained at any
148 point of the track. Although when circumstances permit it may be appropriate to provide
149 sufficient obstacle- and spectator-free spaces for the energy of a car leaving the track out of
150 control to be completely expended.

151 As a general principle, where the estimated impact angle is low a continuous, smooth, vertical
 152 barrier is preferable, and where it is high energy dissipating devices and/or stopping barriers
 153 should be used, combined with a run-off area and deceleration system if there is sufficient
 154 suitable ground available. It is therefore indispensable to provide for sufficient space at such
 155 points in the planning stage. Such areas will be principally situated on the exterior of the
 156 corners and may typically have depths from 30 m to 100 m, according to the approach and
 157 cornering speeds expected on the track.

158
 159 The length of a circuit for the calculation of race distances, race records and classifications is
 160 considered to be that of the centerline of the track. The centerline of the track is the median
 161 line between the left and right edges of the asphalt of the track as delimited by the required
 162 white lines. Particular attention should be paid to this in the case of circuits on city streets.

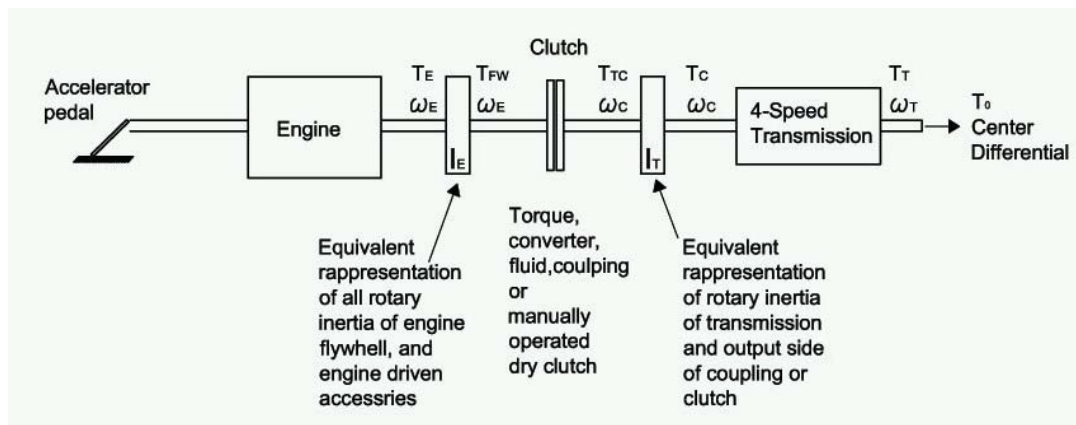
163
 164 **SIMULATION ISSUES**

165
 166 **Vehicle**

167
 168 The vehicle dynamics are based on VDANL/RT that is capable of real time execution at high
 169 update rates (200 Hz or greater) which allows for numerical stability under extreme
 170 maneuvering and road surface input conditions and provides sufficient bandwidth for realistic
 171 steering torque feel. VDANL/RT includes lateral/directional and longitudinal dynamics, tire
 172 forces and aligning torque, wheel spin mode dynamics, and models for the power train and
 173 steering and braking systems. The following figures 1 to 5 have been adapted from Allen et
 174 al. (1998).

175
 176 In Figure 1 the system for central torque and central angular rate generation is shown. The
 177 engine model provides torque as a function of throttle angle, RPM and load. Engine closed
 178 throttle drag torque can also approximate the operation of a Jake brake. Any number of
 179 transmission gears can be simulated based on the positions of gear shift and gear range
 180 controls. The power/drive train is shown in the figure 2. This is the system for torques and
 181 angular rates generation at any single wheel.

182



183
 184 Figure 1 Simulation system for central torque and central angular rate generation
 185

186 The steering system is modeled as a second order dynamic process with inputs provided by
 187 driver steering commands, power steering boost, and tire aligning moments. The steering
 188 system model provides wheel steer angle to the steering axle tire model, and steering wheel
 189 torque commands for steering torque cueing. Moreover the brake system provides torques at
 190 all braking axles based on brake pressure.

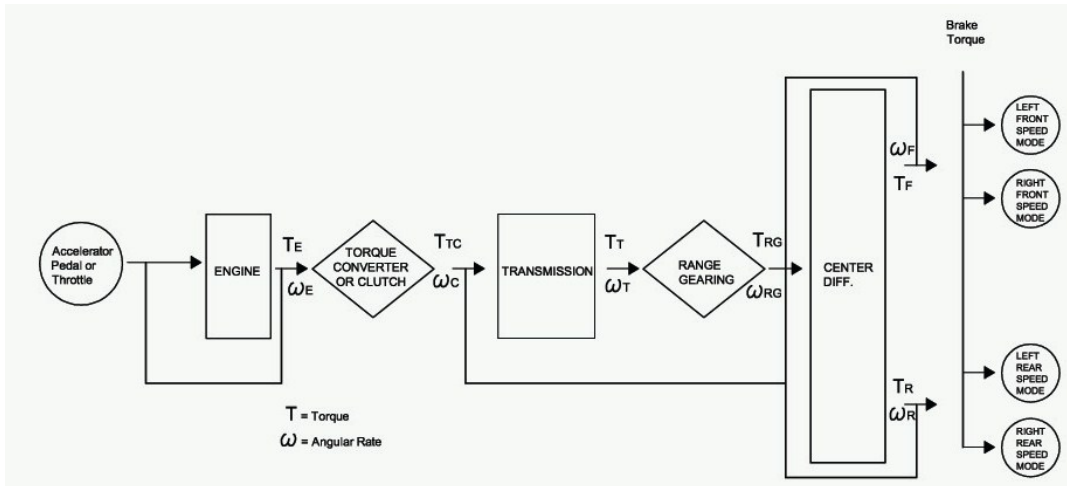
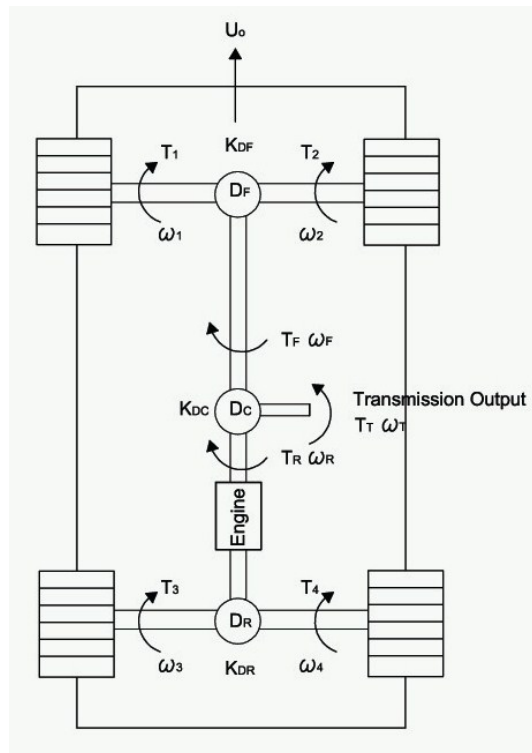


Figure 2 Simulation system for torques and angular rates generation at the wheel

191
192
193
194
195
196
197
198
199
200
201

The brake system model provides for pneumatic delays and generic antilock characteristics based on limiting wheel slip angle to some maximum value. The brake system model also simulates brake lining fade or reduction in coefficient of friction as a function of temperature. Brake temperature is based on a thermodynamic model that accounts for power absorbed minus heat conducted and convected away from the lining. In Figure 3 the system for computation of the dynamical parameters at the single wheels is shown. Figure 4 shows qualitatively as the net engine torque T_E varies as the angular rate at the engine ω_E .



202
203
204
205
206
207
208

Figure 3 Simulation system for computation of the dynamical parameters at the single wheels

The net engine output torque can be specified using a second order equation and the engine characteristics can be defined by the coefficients of this second order equation:

$$Torque = Ep0 + Ep1 \cdot \omega + Ep2 \cdot \omega^2 \quad (2)$$

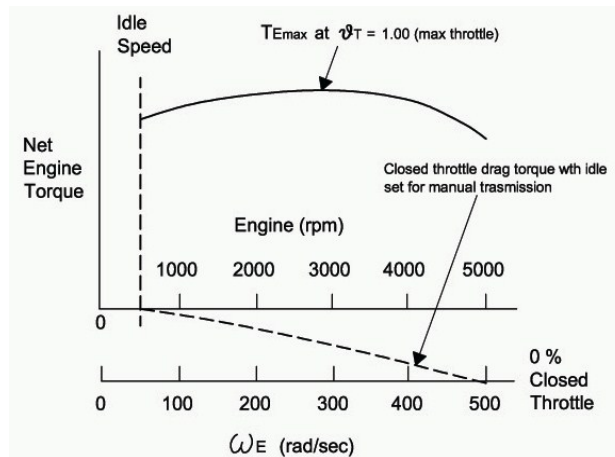


Figure 4 Net engine torque versus the engine angular rate

209
210
211

212 In the power-train parameters settings dialog box $Ep0$ is the “Engine idle gain”, $Ep1$ is the
213 “Linear engine torque gain” and $Ep2$ is the “Second order torque gain”. In the torque map
214 shown above, the engine idle gain sets the value of torque at 0 throttle and corresponds to the
215 torque at the far left where the torque curve and Idle Speed line intersect. The linear engine
216 torque gain sets the slope of the torque curve from the idle speed line to the right. The
217 rounding of the torque curve and eventual drop off is handled by the second order torque gain.
218 As the engine RPM gets higher, the available torque drops off faster.

219

220 The gear ratio KGR_i is set according to the high performing vehicle requirements. The time
221 shift Δt is the time needed for the gear ratio exchange (Figure 5). For simulating a high
222 performing vehicle we have calibrated the parameters (DRT.KE1, DRT.KE2, DRT.KE3), that
223 modulate the torque generated from the engine and transmitted in function of the angular
224 speed rate. The time shift Δt has been reduced to 0.1 seconds, while the maximum value of
225 the angular speed rate (DRT.OMEGAEMAX) has been increased to 2615 rad/sec.

226

227 According to FIA requirements for the vehicle configuration the following standards have
228 been assumed:

- 229 - Minimum weight (full loaded) 620 kg
- 230 - Maximum transversal dimension 1.8 m
- 231 - Maximum vehicle high 0.95 m

232 Other main geometrical characteristics of the vehicle are shown in Figure 6.

233

234 The simulated vehicle maximum speed is about 250 km/h. The possible longitudinal
235 acceleration of the simulated vehicle is 4.5 times lower rather than the possible acceleration of
236 a real F1 vehicle.

237

238 **Circuit geometry**

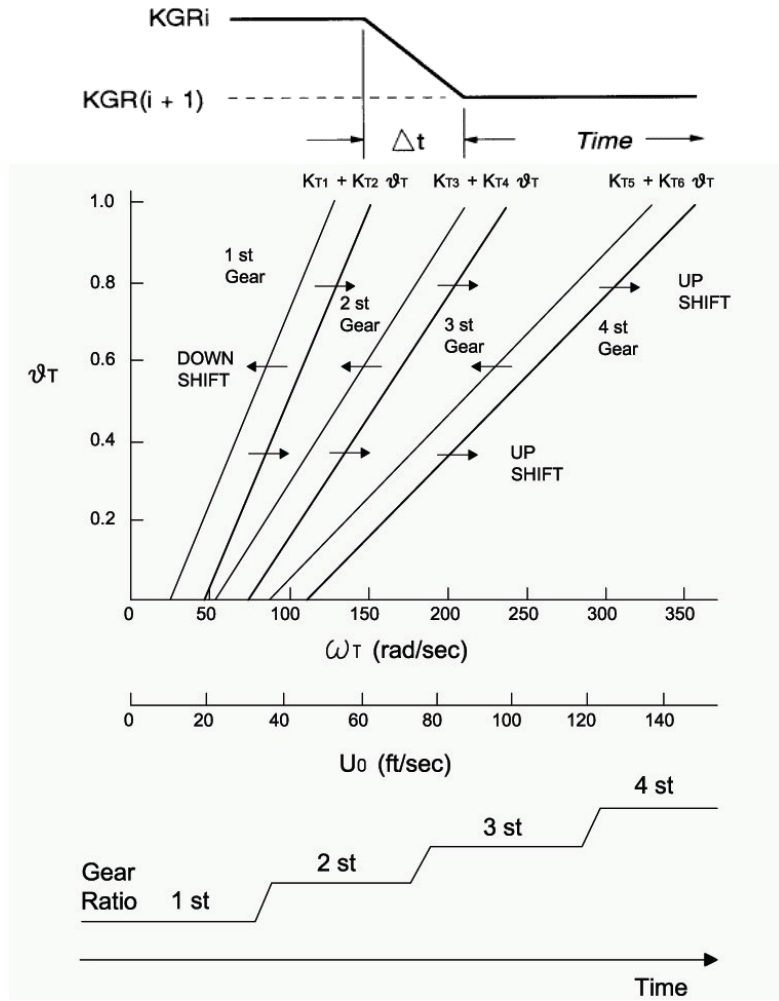
239

240 The circuit can be reproduced in simulation starting from the real geometry. Road section,
241 lanes dimensions, off run zones, signs can be easily implemented as well as the horizontal and
242 vertical alignment through length of tangents, lengths and radii of curves, slopes and vertical
243 radii. In addition the external environment, landscape and skyline are simulated capturing
244 pictures or videos from the reality and generating 3D objects using advanced graphical
245 software.

246

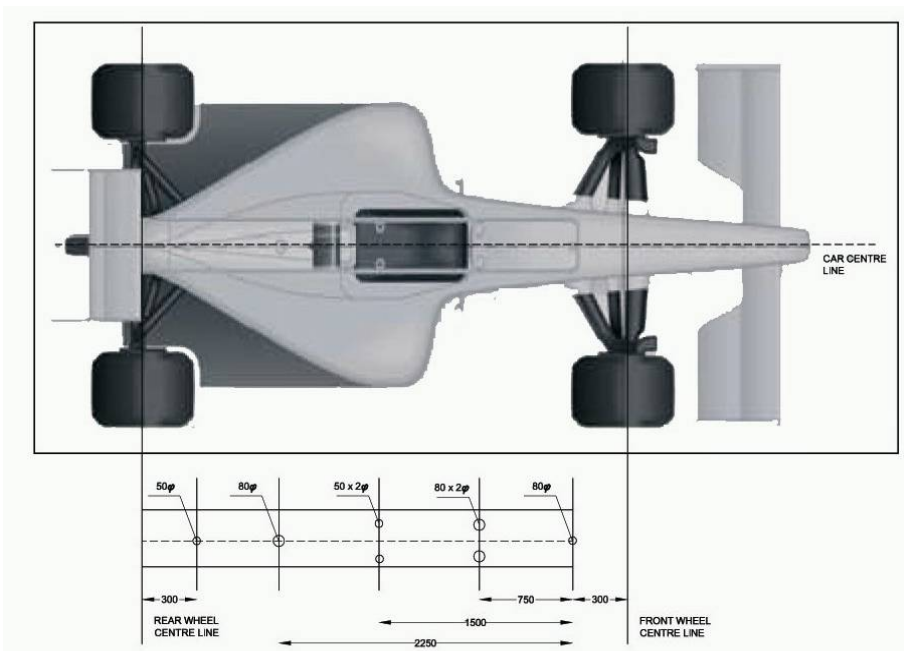
247

248



249
250
251

Figure 5 Time shift for four gear ratios and throttle aperture rate vs angular rate



252
253
254
255

Figure 6 Geometrical characteristics of the vehicle
(adapted from: Formula One World Championship regulations www.fia.com)

256 **Tire-pavement contact**

257

258 The tire model generates lateral and longitudinal tire forces and aligning moments as
259 functions of normal load, slip and camber angle and includes appropriate interactions between
260 these input variables including force saturation.

261

262 The model equations are based on a composite slip formulation, which is basically a quadratic
263 function of lateral and longitudinal slip. Lateral slip is expressed as the ratio of the side slip
264 velocity of the tire patch relative to the longitudinal speed of the tire patch, which is the
265 equivalent of the tangent of the tire patch slip angle. Longitudinal slip is defined as the ratio
266 of the differential tire patch to ground longitudinal velocity divided by the longitudinal
267 velocity of the wheel hub relative to the ground (Allen et al., 1997).

268

269 To reproduce at the possible best the characteristics of a highly performing vehicle, the
270 longitudinal and transversal friction coefficients have been calibrated as well as some specific
271 tire characteristics as stiffness coefficients and lateral and longitudinal slip.

272

273 **CASE STUDY**

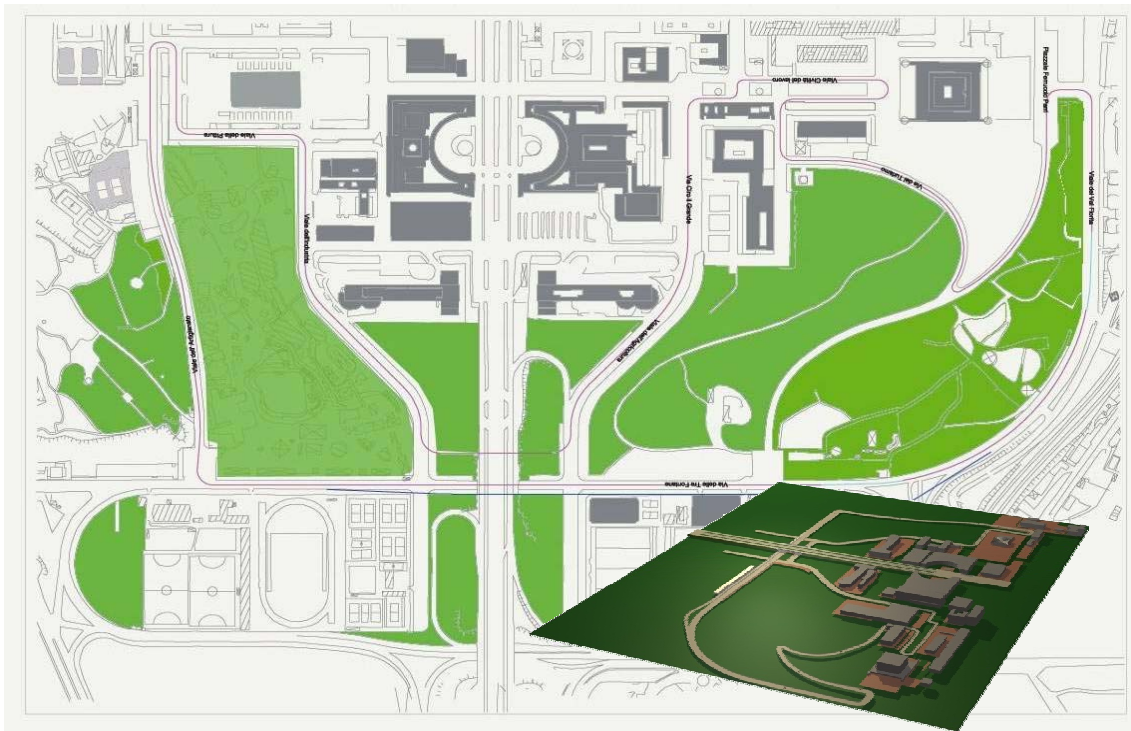
274

275 **The Circuit of Roma**

276

277 In the 2010 the Major of Rome (Italy) has proposed the project for a new Formula 1 GP to be
278 hosted in Rome (Figure 7). The urban circuit is located in the South part of the City (EUR
279 district). The circuit is 6056 m long, the minimum radius of the horizontal curve is 8 m, there
280 are no transition curves, the maximum length of the tangent is 969 m (Figure 8), the
281 maximum longitudinal slope is 3.5% and it is 470 m long (Figure 9). Vertical and horizontal
282 alignments are respectively shown in Figures 8 and 9. The 3D scenario has been generated
283 using advanced graphical software. Three very realistic snapshots are shown in Figure 10.

284



285

286

Figure 7 The test F1 circuit of Rome

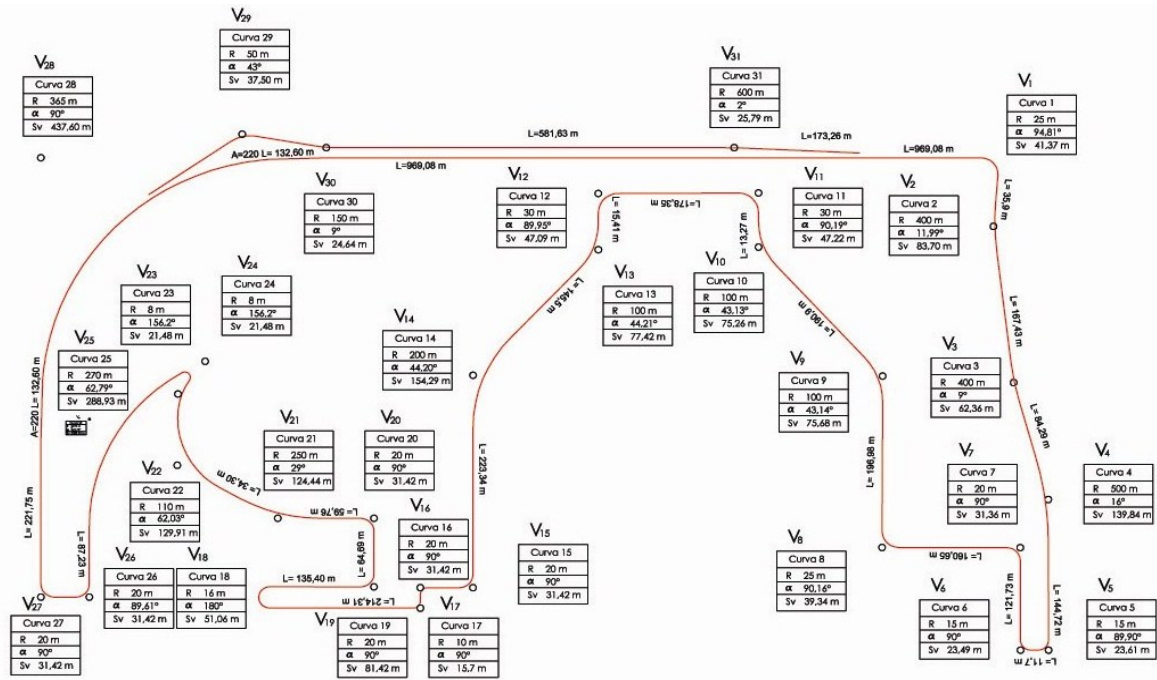


Figure 8 The geometrical characteristics of the test F1 circuit of Rome

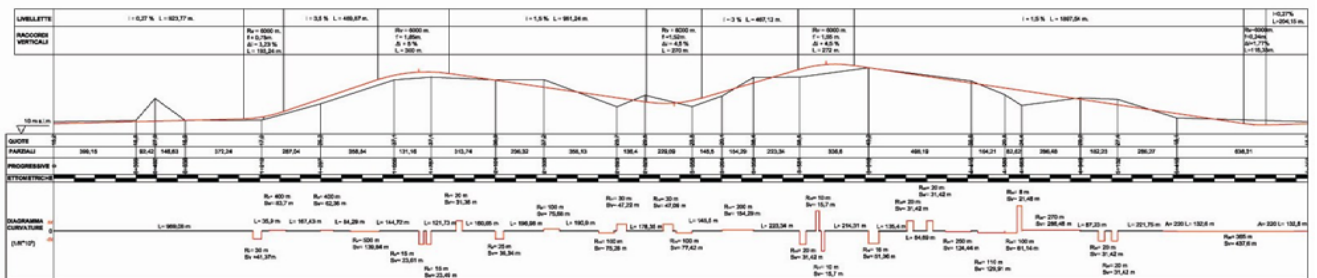


Figure 9 The vertical alignment of the test F1 circuit of Rome

Subjects

The participants have been selected in order to have the very reliable outcomes. With this major aim two subjects who have a significant experience as pilots have been invited to the experiments. One of them has a more relevant experience with the national and international races. After data processing it was evident that this pilot has demonstrated a much more stable performance and behavior during the test, the other experienced much more variable speeds and unstable maneuvers. For the study, considering that this is a preliminary investigation of the simulator capabilities and at this stage no statistical validity is requested, we have assumed the experimental outcomes only from the best pilot.

Tests

In the first phase of the test, the pilot is requested to drive some different scenarios in order to become familiar with the equipment. In the last step of the training the pilot drives on the Formula 1 EUR circuit. The training takes about twenty minutes in total.



Figure 10 Snapshots from the simulation scenario

312
313
314
315
316
317
318
319
320
321
322
323
324
325
326
327
328
329
330
331
332
333
334
335
336
337
338
339

In the simulation that is taken into account for the analysis the pilot is requested to do three separated identical tests. Between two consecutive tests the pilot rests for at least thirty minutes.

In the single test the pilot is requested to drive six laps. Finally 18 laps have driven. The first laps of each test is discharged because the long acceleration phase influences greatly the outcomes. It means that we have 15 laps available for data post processing. Each parameter (speed, accelerations, position,...) is sampled with a step of about five meters.

RESULTS AND DISCUSSION

At the first stage the average speeds for lap have been calculated. In Figure 11 the average speeds for the 15 laps are shown, compared to the maximum and minimum speeds. The average speed of the lap number 7th is the highest 37.461 m/s, the time lap is 161 seconds. The minimum instantaneous speed, 33.270 m/s, is in the 11th lap, the maximum peak speed is 67.656 m/s in the 15th lap.

By investigating the instantaneous speeds along the 7th lap, it is possible to identify the sectors of the circuit where the speed is largely over the average speed over the other laps. In particular these sectors are 4: the 1st at the end of the long tangent leading to the first curve, the 2nd between the curve number 9 and the tangent 10, the 3rd is the tangent 14 to the tangent 15, including the curve 14, and the 4th from the curve 25 to the tangent 23.

Comparing the speed profile observed in the 7th lap to the average speed profile, as in Figure 12, it appears that in the 7th lap the driver has a speed up to 40-45% higher rather than the average.

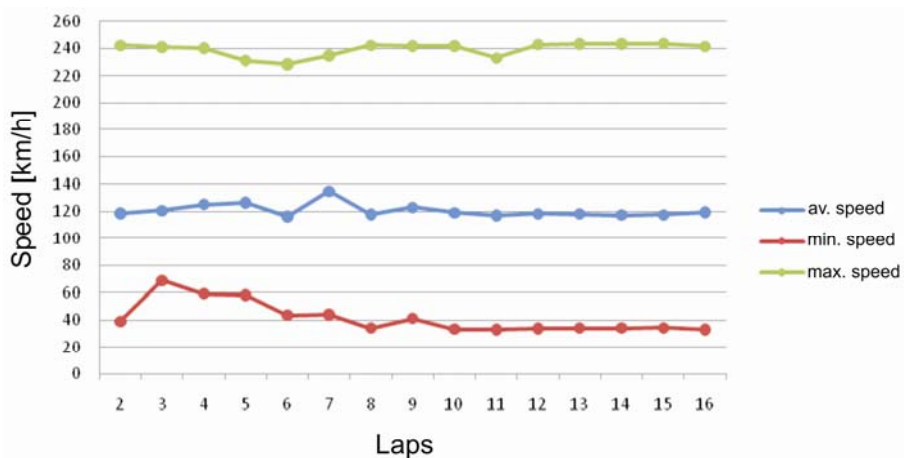
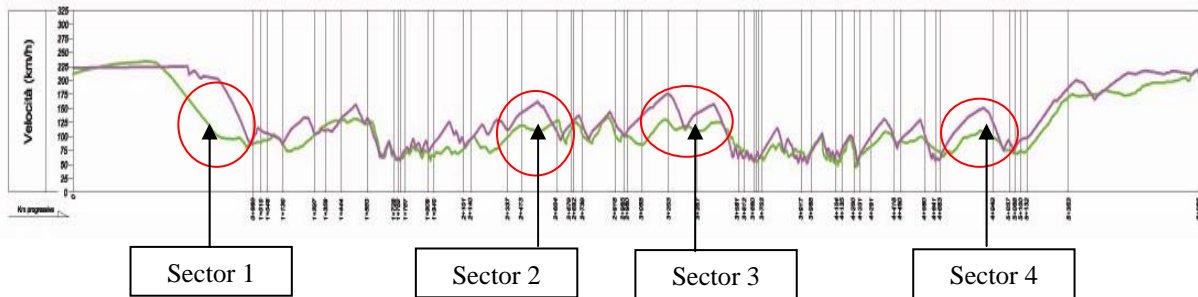


Figure 11 Average speed for the 15 laps

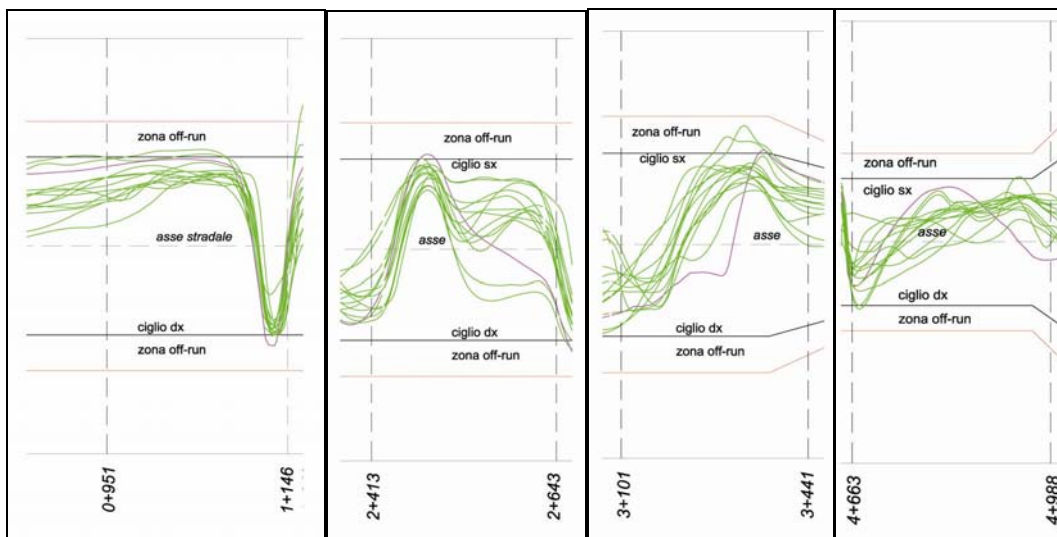
340
341
342

343 For an in depth investigation the trajectories of the vehicle along the lap have been analyzed.
 344 The trajectories of the vehicle in the four sectors for each lap are shown in Figure 13. From
 345 the trajectories geometry it is possible to extract the local curvature of the single trajectory.
 346



347
 348
 349
 350
 351 Figure 12 Comparison between the speed profile observed in the 7th lap and the mean profile
 352
 353

354 The local curvature observed in the 7th lap is compared to the mean local curvature of the
 355 trajectories extended to all the 15 laps for each sector (Figure 14).
 356



357
 358
 359 Figure 13 Trajectories of the vehicle in the four sectors for the 14 laps (green)
 360 compared to the trajectory observed in the 7th lap (red)
 361
 362

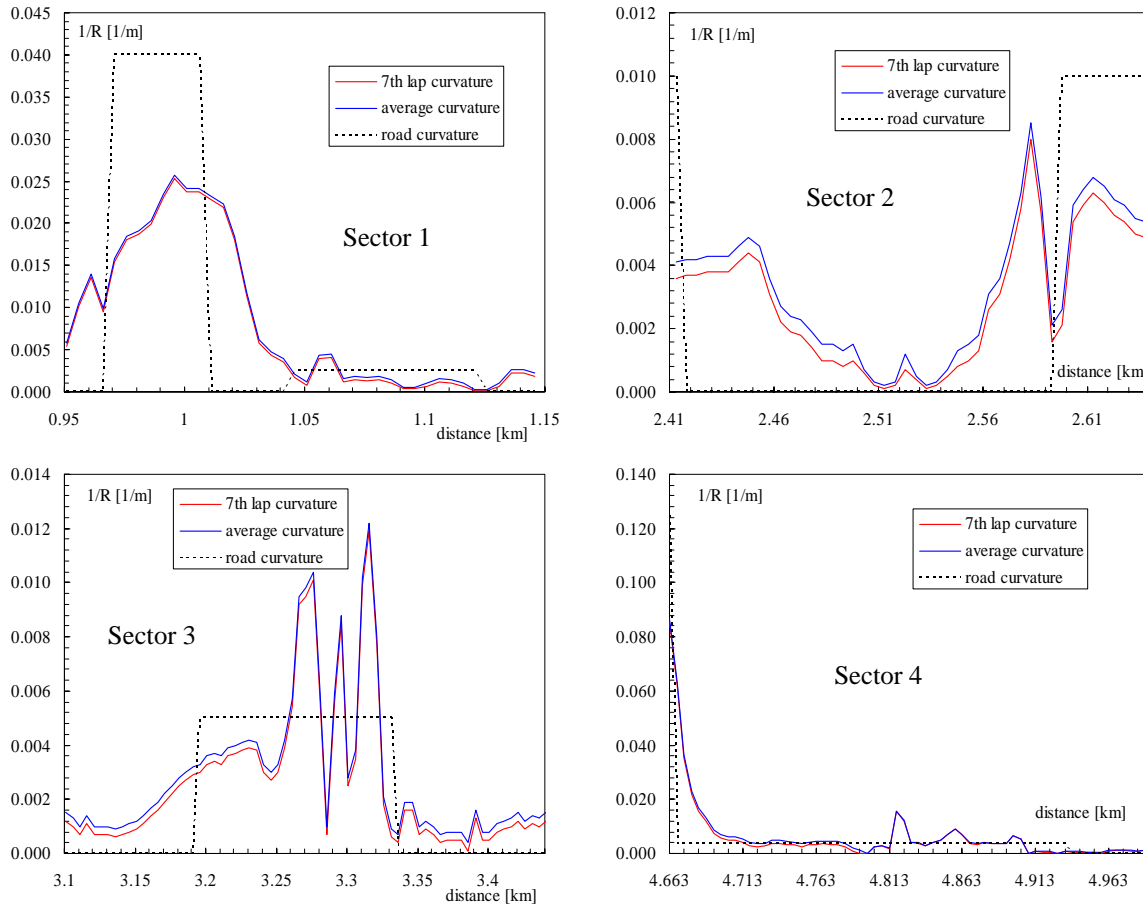
363 Figure 14 shows that the trajectory curvature of the 7th lap is always lower than the mean
 364 trajectory. It means that the vehicle has driven in these sectors of the 7th lap a longer path
 365 rather than the average, however the elapsed time is largely lower in the 7th lap, being the
 366 local speed significantly higher. The trajectory of the vehicle in the 7th lap can be considered
 367 the best compromise between the need for the highest speed and the need for the shorter path.
 368

369 From the simulations output it is possible to extract the values of used friction related to the
 370 available friction at the tire-pavement contact. This analysis can be extended all over the
 371 circuit and to all the four tires of the vehicle. Following this approach the most critical
 372 sections along the circuit have been isolated considering where the rate between used and
 373 available friction at the contact is over 90%. Three sections along the circuit resulted critical:

- 374 - curve 5 – radius 15 m, deviation angle 90°, length 23.61 m,
- 375 - curve 10 – radius 100 m, deviation angle 43°, length 75.26 m,
- 376 - curve 26 – radius 20 m, deviation angle 90°, length 31.42 m.

377
378
379
380
381

It is interesting to note that the curves with minimum radii do not result critical because the speed is very low and consequently the transversal acceleration is limited.



382
383
384
385
386
387
388
389
390
391
392
393
394
395
396
397
398

Figure 14 Local curvature observed in the 7th lap compared to the mean local curvature of the trajectories extended to all the 15 laps

Along the three critical curves it is identified the point where the used/available friction rate is maximum. It results that in the 50% of the cases the maximum rate is observed entering the curve, while braking, in the 32% of the cases in exiting from the curve and 18% in the center of the curve. Among the three, the most critical case resulted the curve 5.

Figure 15 shows the rate between the used and available friction all along the curve over a two dimensional map, for the four wheels. From Figure 15 it results as reasonably expected that the most critical wheel is the rear right wheel, because the weight results lower for combined effect of the centrifugal force and of the inertia for braking.

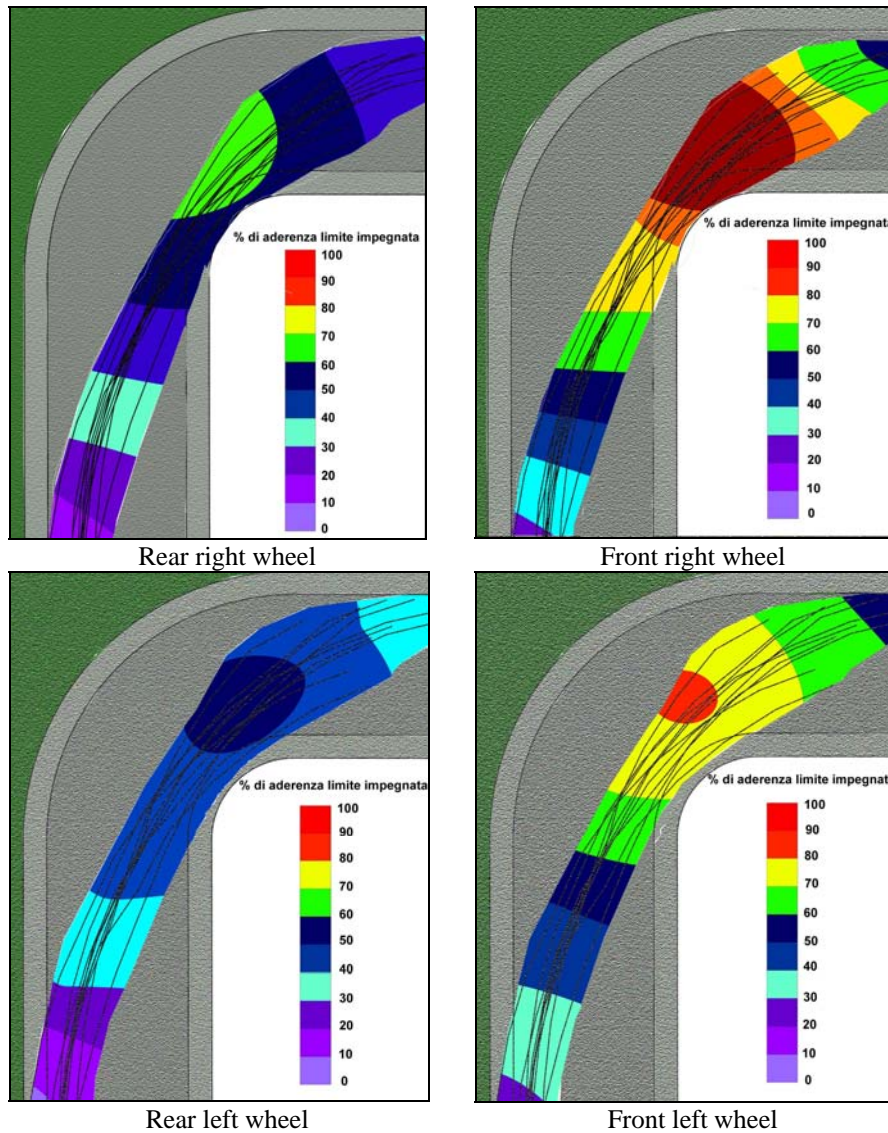


Figure 15 Two dimensional map of the used/available friction rate all along the curve for the four wheels

399
 400
 401
 402
 403
 404
 405
 406
 407
 408
 409
 410
 411
 412
 413
 414
 415
 416
 417

CONCLUSION

The outcomes of the study demonstrate that simulator is very promising for geometry optimization of the circuit according to the pilots trajectories and to the best performed laps as well as for the pilot training. Finally it has to be noted that the performances of the available simulators should be mostly increased to reproduce more adequately the characteristics of the F1 vehicles, especially regarding the acceleration, in order to carry out more realistic tests.

REFERENCES

Allen, R.W., Chrstos, J.P., and Rosenthal, T.J. (1997). "A tire model for use with vehicle dynamics simulations on pavement and off-road surfaces", *Vehicle System Dynamics*, 27, 318-321.

418 Allen, R.W., Rosenthal, T.J., Aponso, B.L., Klyde, D.H., Anderson, F.G., Hougue, J.R., and
419 Chrstos, J.P. (1998). "A low cost PC based driving simulator for prototyping and Hardware-
420 in-the-Loop Applications". SAE (Society of Automotive Engineers) paper 98-0222.
421

422 Bella, F. (2008). "Driving Simulator for Speed Research on Two-Lane Rural Roads",
423 *Accident Analysis and Prevention*, 40, 1078-1087.
424

425 Bella, F. (2009). "Can Driving Simulators Contribute to Solving Critical Issues in Geometric
426 Design?", *Transportation Research Record*, 2138, 120-126.
427

428 Benedetto, A., de Angelini, A., di Renzo, D., Guerrieri, F., and Markham, S. (2002). "About
429 the Standards of a Driving Simulation for Road Engineering: A New Approach", *Proceedings
430 of the Seventh International Conference Applications of Advanced Technologies in
431 Transportation* ASCE, 704-711.
432

433 Godley, S.T., Triggs, T.J., and Fildes, B.N. (2002). "Driving Simulator Validation for Speed
434 Research", *Accident Analysis and Prevention*, 34, 589-600.
435

436 Hughes, R. (2005). "Research Agenda for the Application of Visualization to Transportation
437 Systems", *Transportation Research Record*, 1937, 145-151.
438

439 Kaptein, N.A., Theeuwes, J., and Van der Horst, R. (1996). "Driving Simulator Validity:
440 Some Considerations", *Transportation Research Record*, 1550, 30-36.
441

442 Klee, H., Bauer, C., Radwan, E., and Al-Deek, H. (1999). "Preliminary Validation of Driving
443 Simulator Based on Forward Speed", *Transportation Research Record*, 1689, 33-39.
444

445 Trentacoste, M. F. (2008). "Integrating Actual Road Design into Highway Driving Simulators
446 for Research, Design, and Consumer Information Applications", *Advances in Transportation
447 Studies: An International Journal*, 14, 7-16.
448

449 Yan, X., Abdel-Aty, M., Radwan, E., Wang, X., and Chilakapati, P. (2008). "Validating a
450 Driving Simulator Using Surrogate Safety Measures", *Accident Analysis and Prevention*, 40,
451 274-288.
452
453